Fusion of $^{28}Si + ^{28}Si$

S. B. DiCenzo* and J. F. Petersen†
A. W. Wright Nuclear Structure Laboratory, Yale University, New Haven, Connecticut 06511

R. R. Betts
Argonne National Laboratory, Argonne, Illinois 60439

(Received 16 September 1980)

The energy dependence of the fusion cross section for $^{28}Si + ^{28}Si$ has been studied over the bombarding energy range 80–140 MeV. The gross features of these cross sections are compared with the expectations of entrance channel models and with the results of time-dependent Hartree Fock calculations. A comparison with similar data for the $^{32}S + ^{24}Mg$ and $^{16}O + ^{40}Ca$ systems gives results which are not inconsistent with a compound nucleus limitation to fusion at high energies. A search for fusion oscillations similar to those found in lighter systems provides some evidence for their occurrence in the $^{28}Si + ^{28}Si$ system.

[NUCLEAR REACTIONS $^{28}Si + ^{28}Si$; E_{lab} = 80–140 MeV measured evaporation residues, deduced $\sigma_{fus}(E)$. Compared entrance channel, TDHF, and yrast limit models.]

I. INTRODUCTION

There is considerable interest in the process whereby two heavy ions fuse, forming a composite system whose mass and charge equal the sum of those of the target and projectile. The systematics of the gross energy dependence of this process is by now quite well established and, at least in principle, can be accounted for by models which depend on the nature of the ion-ion potential and the dissipative processes occurring during the collision. On a more detailed level, however, there are several features of the fusion process which remain unexplained. For example, the occurrence of broad oscillations in the excitation functions for several light systems ($^{12}C + ^{12}C$, $^{12}C + ^{16}O$, etc.) is a feature which apparently lies outside the scope of the fusion models currently available.[1] To date, this phenomenon has been demonstrated for only a limited number of systems, and the range of nuclear systems for which it occurs remains to be determined.

In this paper we present data for the fusion of $^{28}Si + ^{28}Si$ obtained from three separate measurements. In the first of these, the gross features of the energy dependence of the fusion cross section were determined by a measurement of the evaporation residue cross section using an ion chamber telescope. A more detailed measurement was then made, using the same detection system, in a search for oscillations as a function of energy similar to those observed for lighter systems. Finally, a more careful search for oscillations, which included identification of the final products through their characteristic γ rays, was also made.

The choice of the $^{28}Si + ^{28}Si$ system for this work was motivated largely by empirical observation that fusion oscillations occur most markedly in systems where the target and projectile are identical alpha-particle nuclei. The $^{28}Si + ^{28}Si$ system, which provides a significant change in mass from those systems in which fusion oscillations have previously been observed, is therefore a natural choice for study.

There has been little previous experimental work on the fusion of $^{28}Si + ^{28}Si$. Medsker *et al.*[2] have measured the yields of gamma rays produced in this reaction at bombarding energies ranging from near the Coulomb barrier to 90 MeV. The target used, however, was 4 MeV thick to the beam, rendering that study unsuitable as a test for the existence of oscillatory fusion cross sections.

In a theoretical work[3] which has appeared recently, the results of time-dependent Hartree-Fock (TDHF) calculations of the fusion cross section for $^{28}Si + ^{28}Si$ have provoked much interest in that they predict the occurence of a fusion window, with the lower partial waves not contributing to the fusion cross section at higher energies. While the present data do not in any sense test this prediction, they do for the first time make possible a comparison with experiment of the overall features of the TDHF calculated cross sections.

Finally, recent data[4] for the elastic scattering of $^{28}Si + ^{28}Si$ have revealed striking, resonancelike behavior. This behavior suggests the appropriateness of a surface-transparent type of optical po-

tential for this system—increasing the expectation that the fusion cross section may also show resonancelike behavior.

II. EXPERIMENTAL METHOD

As mentioned above, the data presented in this paper are the result of three separate experiments. In the first of these an ion chamber telescope was used to detect evaporation residues resulting from the fusion process. A beam of ^{28}Si ions from the Yale University MP tandem was used to bombard a 10 μg/cm^2 ^{nat}Si metal target (92% ^{28}Si) deposited on a 10 μg/cm^2 carbon backing. A ΔE-E spectrum obtained at a bombarding energy of 100 MeV and at a laboratory angle of 7° is shown in Fig. 1. Also shown is a similar spectrum taken with a carbon target, illustrating the clean separation of the ^{28}Si + ^{28}Si fusion evaporation residues from other reaction products. The energy spectrum resulting from the projection of the Si + Si fusion events onto the total energy axis is shown in Fig. 2; no low-energy cutoff is evident in these data. Similar spectra were obtained at angles between 3° and 20° and at bombarding energies of 80, 90, 100, 120, and 140 MeV. A fixed monitor detector was used to provide the angle-to-angle normalization.

The angular distributions of the evaporation

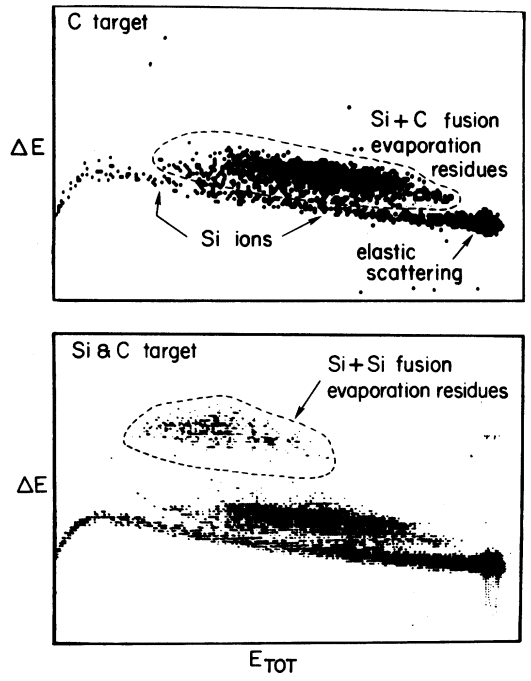

FIG. 1. ΔE-E spectra obtained with the ion chamber telescope at θ_{lab} = 7°, E_{lab} = 100 MeV, for (above) a carbon target and (below) a target consisting of ^{nat}Si deposited onto a similar carbon backing.

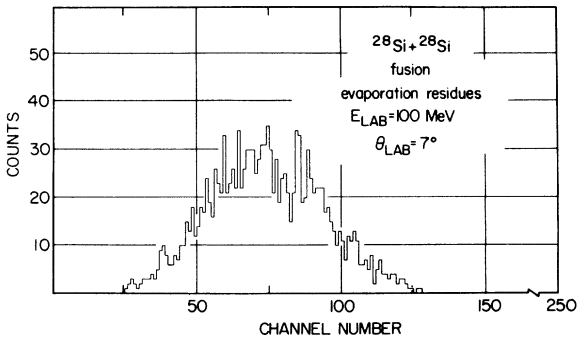

FIG. 2. The projection onto the E axis of the Si + Si fusion products indicated in the lower part of Fig. 1.

residues are shown in Fig. 3, where the absolute cross section scale was obtained by normalizing to the simultaneously measured angular distributions for the elastic scattering of Si + Si, for which

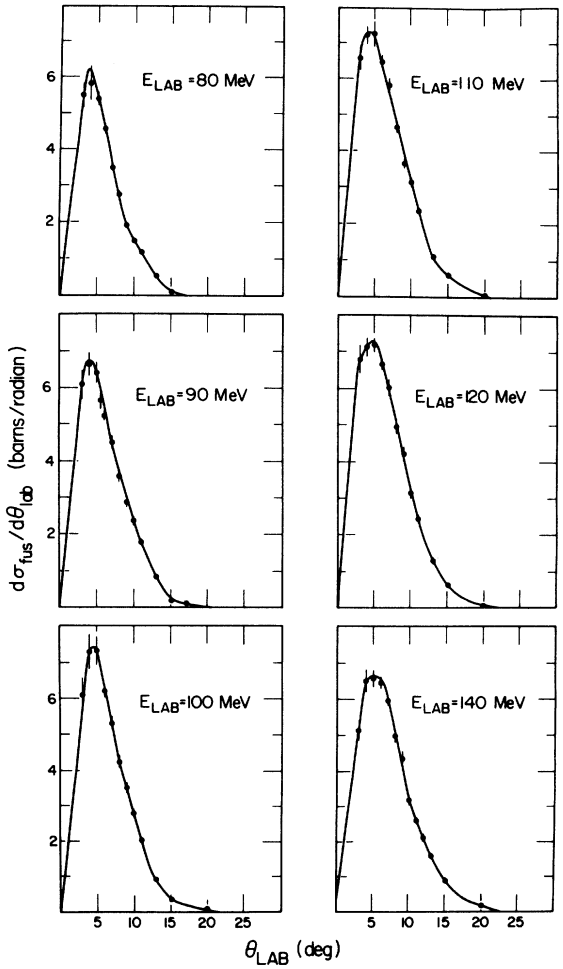

FIG. 3. Angular distributions of the fusion products. These were integrated to obtain the values of σ_{fus} (E), the total cross section for fusion.

the cross section reaches the Coulomb value at forward angles. The absolute uncertainty in the values of the integrated cross sections obtained from these angular distributions, is estimated to be ±5%. These values are listed in Table I.

For the second experiment, the ion-chamber telescope was fixed at 5° in the scattering chamber and used to measure the evaporation residue cross section at 1 MeV intervals over the bombarding energy range 100 to 140 MeV. The following procedure was used to correct the energy to energy normalization for small changes in the scattering angle, and to preclude the influence of systematic effects due to, for example, variation in the target thickness and in the charge integration. The target used consisted of ^{nat}Si and ^{89}Y evaporated as a mixture onto a thin carbon backing. As both materials have quite similar vapor pressures the ratio of the two should be constant over the area of the target. Two monitor detectors placed at ±15° relative to the beam axis were then used to measure the elastic scattering yield from the ^{89}Y in the target, which at this angle follows the Rutherford scattering law over the entire energy range studied. The total yield therefore provided a monitor of the target thickness while the ratio of the yields in the two detectors provided a measure of the mean scattering angle, and therefore of the mean beam angle. The sensitivity of this method is such that a shift of 0.1° in the mean beam angle produced a change of 10% in the ratio of the two elastic scattering yields. This information was then used to correct the measured fusion yield according to the angle dependence of that yield as determined in the first experiment. The fusion yields were obtained as described for the first experiment, and are shown in Fig. 4.

Lastly, an experiment in which gamma-ray yields from the fusion evaporation residues were detected was performed. In this case, the target consisted of a uniform 40 $\mu g/cm^2$ layer of Si metal evaporated onto a thick gold backing. The current integration was then taken directly from the target, which was biased to +1 kV and surrounded by an electron suppression grid at −1 kV. The gamma rays were detected in a 65 cm^3 Ge(Li) detector placed 5 cm from the target at 90° to the beam axis. A spectrum obtained at a bombarding energy of 92 MeV is shown in Fig. 5, with the individual lines indicated by their energies. The transitions were identified according to the information found in the Nuclear Data Sheets and in the literature.[5] The gamma rays observed were essentially those reported in Ref. 2, except for the transitions in ^{47}V and ^{49}V, which were not included in that study. Spectra were

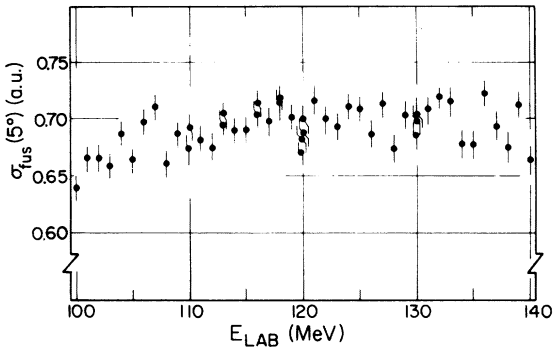

FIG. 4. Yields of $^{28}Si + Si$ fusion products at $\theta_{lab} = 5°$, corrected for variations in target thickness, beam angle, and total beam flux.

measured at 1 MeV steps between 80 and 100 MeV bonbarding energy. The integrated yields were normalized from energy to energy assuming a smooth energy dependence of the Coulomb excitation yields from the Au target backing. This normalization procedure thus corrects for dead time effects as well as uncertainties in the charge integration. To reduce random errors the yield of each residual nucleus was then defined as a suitably weighted mean of the yields of several gamma rays from that nucleus, corrected for side feeding and branching. These gamma rays are listed in Table II. The absolute cross section scale was obtained by normalizing the sum of these yields at $E_{lab} = 80$ MeV to the value obtained in the first experiment. The resulting cross sections are shown in Fig. 6.

III. DISCUSSION

A. Gross features of fusion cross sections

The cross sections obtained from the fusion angular distribution measurements are shown in Fig. 7, plotted as a function of $1/E_{c.m.}$. Also shown on this figure are the data of Ref. 2 which are plotted as open circles. As no absolute cross section scale was quoted by those authors, their relative cross section data were normalized to the 80 MeV data point from the present work. Their highest energy data point was not included in this normalization owing to the previously mentioned neglect of gamma rays from ^{47}V and ^{49}V. The present gamma ray work (see Fig. 6) indicates a cross section approaching 100 mb for these two nuclei at 90 MeV, thus accounting for the apparent discrepancy between the two sets of data at this energy.

The dashed line in Fig. 7 is the result of a linear least squares fit to the data below 100 MeV, excluding the 90 MeV point mentioned above, using the expression

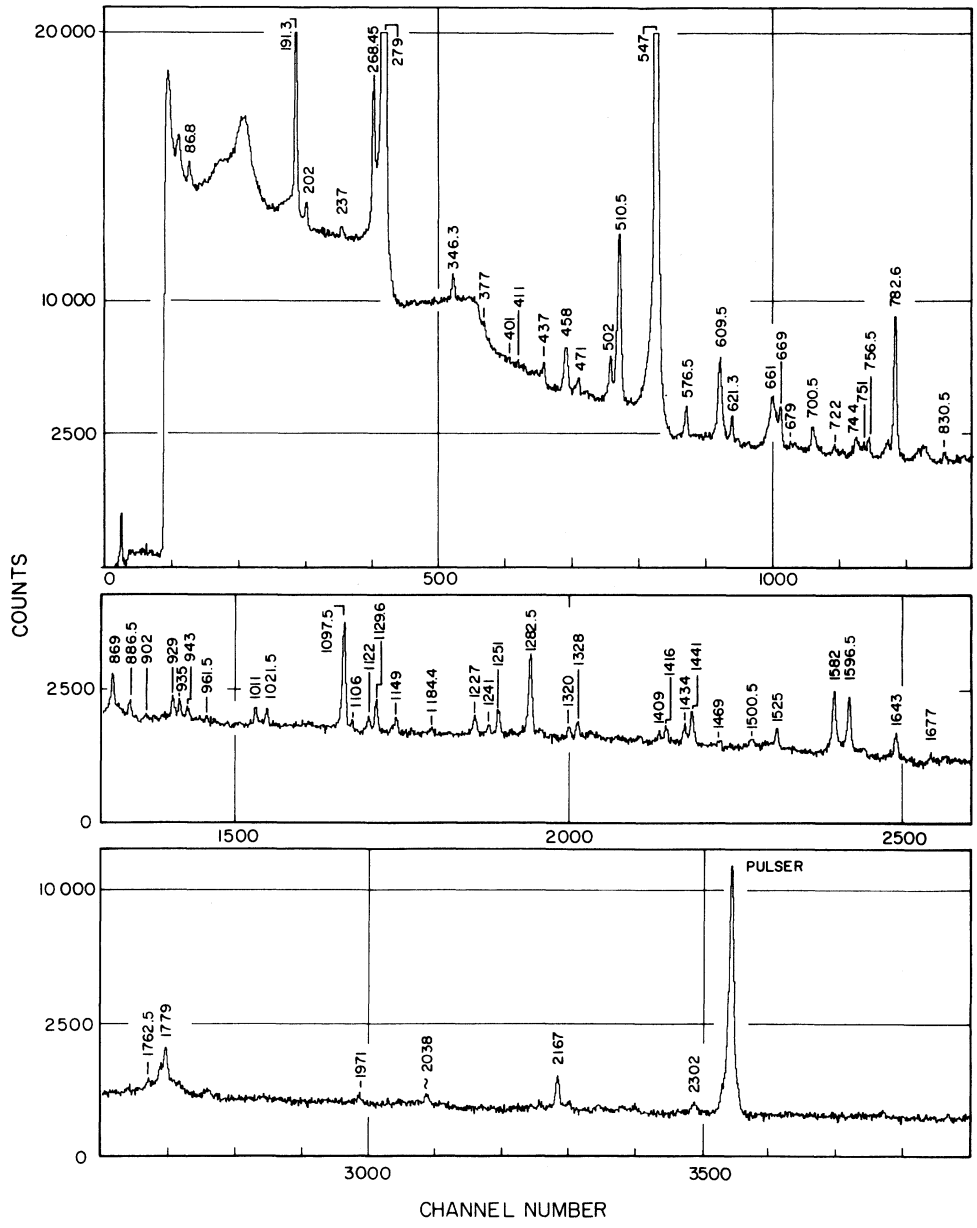

FIG. 5. Spectrum of gamma rays resulting from ^{28}Si + Si reactions at a bombarding energy of 92 MeV. The energy (in keV) of each of the more prominent peaks is indicated.

$$\sigma_{fus} = \pi R_B^2 (1 - V_B/E) \quad (1)$$

as suggested by Glas and Mosel.[6] The values obtained for the two parameters in this expression are $R_B = 9.08 \pm 0.25$ fm and $V_B = 29.6 \pm 0.5$ MeV which are to be compared with the values $R_B = 9.26 \pm 0.08$ fm and $V_B = 30.5 \pm 0.3$ MeV obtained from a quarter point analysis of ^{28}Si + ^{28}Si elastic scattering data[7] at 80, 100, and 120 MeV. At energies above 100 MeV, the measured fusion cross sections begin to fall below the expected total reaction cross section, the difference being nearly 500 mb at 140 MeV bombarding energy. Within the model of Glas and Mosel,[6] it is appropriate to parametrize the data in this region according to the expression

$$\sigma_{fus} = \pi R_{cr}^2 (1 - V_{cr}/E) . \quad (2)$$

TABLE I. Total cross sections for $^{28}Si + ^{28}Si$ fusion.

E_{lab} (MeV)	σ_{fus} (mb)
80	701 ± 20
90	817 ± 26
100	946 ± 35
110	1003 ± 40
120	1040 ± 32
140	1067 ± 35

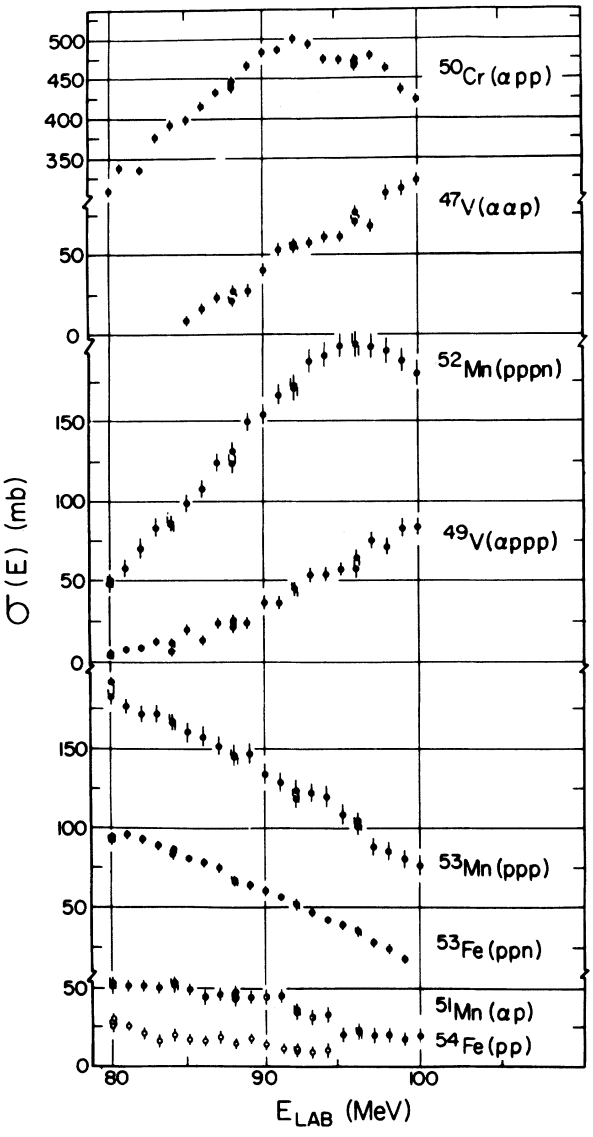

FIG. 6. Cross sections for individual evaporation residues as determined from the yields of their characteristic gamma rays. Note that the scale for the ^{50}Cr data is compressed relative to that for all other nuclei.

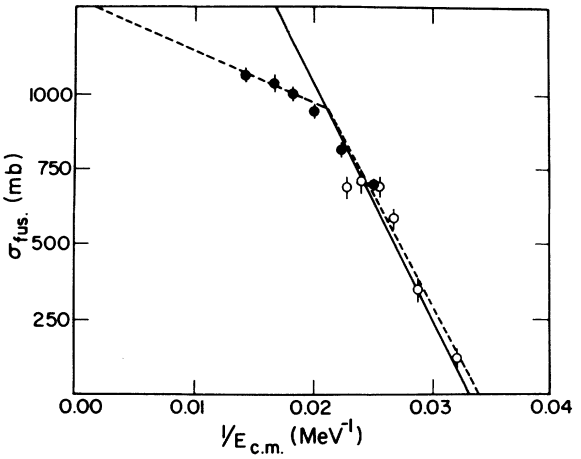

FIG. 7. The fusion cross section $\sigma_{fus}(1/E_{c.m.})$ for $^{28}Si + ^{28}Si$ as measured in the present work (closed circles) and as reported in Ref. 2 (open circles), compared with the linear fits described in the text (dashed lines) and with the total reaction cross section determined from a quarter-point analysis of elastic scattering data (solid line).

The present data are not sufficient to allow the reliable extraction of both these parameters. If, however, we take a value for

$$R_{cr} = 1.07(28^{1/3} + 28^{1/3}) = 6.50 \text{ fm}, \quad (3)$$

we obtain $V_{cr} = 13.7 \pm 1.8$ MeV by fitting to the data points for energies of 100 MeV and above. This value for R_{cr} is consistent with the systematics of measured fusion cross sections.

Theoretical fusion cross sections, calculated using the TDHF approximation,[3] are compared with the experimental values in Fig. 8. The calculated values are shown as data points with error bars corresponding to the uncertainties introduced by the use of the sharp cutoff approximation in the calculations. The experimental values are indicated by the straight lines corresponding to the above Glas and Mosel parametrization over the energy range for which data exist. The overall agreement is reasonable except that the calculated values exceed the average experimental behavior by approximately 15% over the entire energy range. It is likely that this discrepancy arises from the inadequate treatment of the microscopic structure of the two colliding nuclei through the use of the "filling approximation" which assumes that the valence nucleons in the ^{28}Si ground state are distributed equally among the $1d_{5/2}$, $2s_{1/2}$, and $1d_{3/2}$ shell model orbitals.[8] We note that the present results provide no evidence for or against the existence of a lower angular momentum cutoff in the fusion process which underlies the extremely low cross section calculated

TABLE II. Summary of transitions included in the determination of the cross sections for individual final nuclei.

Residual nucleus	Photon energy (keV)	Transition
^{54}Fe	412	$6^+ \rightarrow 4^+$
	1408.5	$2^+ \rightarrow 0^+$(g.s.)
^{53}Fe	701	$(\frac{19}{2})^- \rightarrow \frac{11}{2}^-$
	1012	$\frac{11}{2}^- \rightarrow \frac{9}{2}^-$
	1328	$\frac{9}{2}^- \rightarrow \frac{7}{2}^-$
^{53}Mn	1441	$\frac{11}{2}^- \rightarrow \frac{7}{2}^-$ (g.s.)
^{52}Mn	621.5	$9^+ \rightarrow 8^+$
	869	$7^+ \rightarrow 6^+$(g.s.)
^{51}Mn	237	$\frac{7}{2}^- \rightarrow \frac{5}{2}^-$ (g.s.)
^{50}Cr	610	$11^+ \rightarrow 10^+$
	783	$2^+ \rightarrow 0^+$(g.s.)
	1098	$4^+ \rightarrow 2^+$
	1283	$6^+ \rightarrow 4^+$
^{49}V	1021	$\frac{11}{2}^- \rightarrow \frac{7}{2}^-$
	1240	$\frac{15}{2}^- \rightarrow \frac{11}{2}^-$
^{47}V	1149	$\frac{11}{2}^- \rightarrow \frac{7}{2}^-$
	1320	$\frac{15}{2}^- \rightarrow \frac{11}{2}^-$

for fusion at the highest bombarding energies.

Data exist for two other systems having the same compound nucleus as ^{28}Si + ^{28}Si, namely ^{32}S + ^{24}Mg (Ref. 9) and ^{16}O + ^{40}Ca.[10] It has been suggested[11] that the heavy-ion fusion cross section at high energy may be limited by the yrast line of the compound nucleus. It was concluded,[11] on the basis of calculated yrast lines, that this is not the case. This question is, however, best answered empirically. A comparison of the results for these three systems is therefore of some interest as it in principle allows a distinction between possible mechanisms of the fusion process at high energies. The way in which this is accomplished is by extracting from the measured fusion cross sections the values of the maximum angular momentum leading to fusion (l_{fus}). If the limitation to fusion at high energies is indeed the yrast line of the compound nucleus, for energies above the fusion turn over, the values of l_{fus} should depend only on the excitation energy in the compound nucleus and not on the specific entrance channel. The simplicity of this means of testing the yrast line limitation hypothesis is, however, clouded by some uncertainty in the extraction of

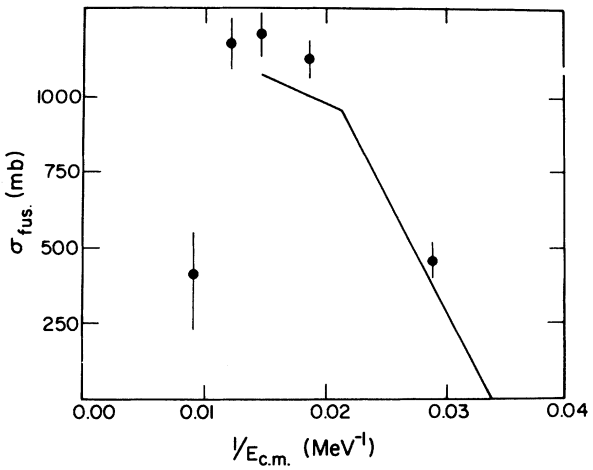

FIG. 8. Fusion cross sections from the TDHF calculations of Ref. 3, compared with the experimental values (solid curve).

l_{fus}. This uncertainty arises as a result of the way in which angular momentum is treated in the sharp cutoff expression for fusion cross sections

$$\sigma_{fus} = \pi \lambda^2 \sum_{l=0}^{l_{fus}} (2l+1), \tag{4}$$

where on one hand l is treated as a discrete quantal variable in the evaluation of the sum in Eq. (4) and yet on the other hand is allowed to assume noninteger values when it is evaluated from the measured fusion cross sections. It therefore seems sensible in the present situation to treat l as a classical continuous variable and replace the sum in Eq. (4) by an integral over l which results in the expression

$$\sigma_{fus} = \pi \lambda^2 l_{fus}(l_{fus}+1). \tag{5}$$

In order to express the uncertainty in this procedure we have associated an error of $\pm 1\hbar$ or the experimental error, whichever is greater, with the values of l_{fus} extracted from the data. These values for ^{28}Si + ^{28}Si, ^{32}S + ^{24}Mg, and ^{16}O + ^{40}Ca are shown in Fig. 9 plotted as a function of excitation energy in ^{56}Ni, the compound nucleus. We see that, for excitation energies above approximately 50 MeV, the values of l_{fus} from the difference entrance channels are essentially indistinguishable from one another. For the purposes of orientation the solid curve shows the yrast line calculated assuming the moment of inertia to be that of a rigid sphere of radius $1.25(56)^{1/3}$ fm. We note, however, that the true yrast line almost certainly lies considerably below this line. The observation that the three different entrance channels have essentially identical values of l_{fus}

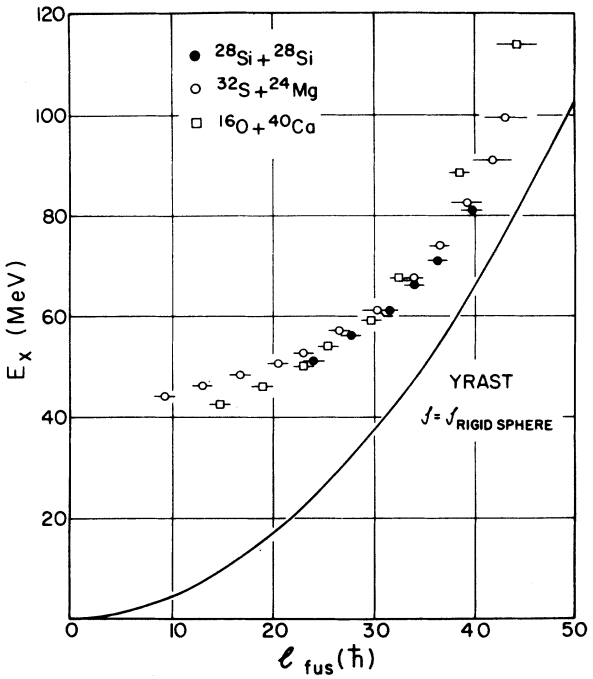

FIG. 9. Values of l_{fus} determined as described in the text shown as a function of compound nucleus excitation energy.

for the same excitation energy, while not proving the existence of an yrast limit to fusion in the present case, does not exclude the possibility. The question is then whether these data are or are not consistent with the expectation of entrance channel models of the fusion cross section. In Table III we list the values of V_{cr} and R_{cr} obtained from Glas and Mosel fits to the high energy fusion data for these three systems. Also listed are the values of the Coulomb potential evaluated at the critical radius $[V_{Coul}(R_{cr})]$ and the value of the nuclear potential $[V_{nuc}(R_{cr})]$ defined as the difference between V_{cr} and V_{Coul}. We note that the value of $V_{nuc}(R_{cr})$ for $^{28}Si + ^{28}Si$ is considerably smaller than for either $^{32}S + ^{24}Mg$ or $^{16}O + ^{40}Ca$. This result is in contrast with expectations for the values of $V_{nuc}(R_{cr})$ calculated using, for example, the Bass potential[12]

$$V_{nuc} = -a_s A_1^{1/3} A_2^{1/3} \frac{d}{R_{cr}} \tag{7}$$

with $a_s = 17$ MeV and $d = 1.5$ fm which are noted in Table III. We see that this prescription predicts rather small variations in $V_{nuc}(R_{cr})$ for the three systems, in contrast to the experimental results. It should be pointed out, however, that the value of V_{cr} for $^{28}Si + ^{28}Si$ is based on rather limited data and the conclusions of this analysis, although consistent with a yrast limit to the fusion process and seemingly inconsistent with a static entrance channel limitation, must therefore be considered very tentative. More high energy data are required in order to verify these conclusions.

B. Evidence for fusion oscillations

The evaporation residue function data presented in Fig. 4 show little evidence for structure similar to that seen in lighter systems. The data do allow the observation that such structure, if it exists, must represent at most 5% of the fusion cross section, and will thus be very difficult to detect in an experiment measuring the total cross section. If, however, the structure appears preferentially in certain evaporation channels, as is the case in the lighter systems, an experiment which identifies such channels will be more likely to reveal even a weak structure. This possibility provided the motivation for the gamma ray experiment, which, although poorly suited to the measurement of absolute cross sections, is well suited to the above purpose.

The gamma ray cross sections shown in Fig. 6 do indeed show some evidence for energy dependent structure. Within the quoted errors, the data for the majority of final nuclei are consistent

TABLE III. Potential parameters for fusion reactions leading to ^{56}Ni.

Channel	V_{cr} (MeV)	R_{cr} (fm)	$V_{Coul}(R_{cr})$ (MeV)	$V_{nuc}(R_{cr})$ (MeV)	$V_{Bass}(R_{cr})$[a] (MeV)
$^{28}Si + ^{28}Si$[b]	13.7 ± 1.8	6.50[c]	43.4	−29.7 ± 1.8	−36.17
$^{32}S + ^{24}Mg$[d]	0.9 ± 3.1	5.89 ± 0.15	46.9	−46.0 ± 3.1	−39.65
$^{16}O + ^{40}Ca$[e]	−2.7 ± 8.5	6.00 ± 0.40	39.9	−42.6 ± 8.5	−36.63

[a] Calculated using the expression given in the text.
[b] Present work.
[c] Fixed by assuming $R_{cr} = 1.07(28^{1/3} + 28^{1/3})$ fm.
[d] Reference 9.
[e] Reference 10.

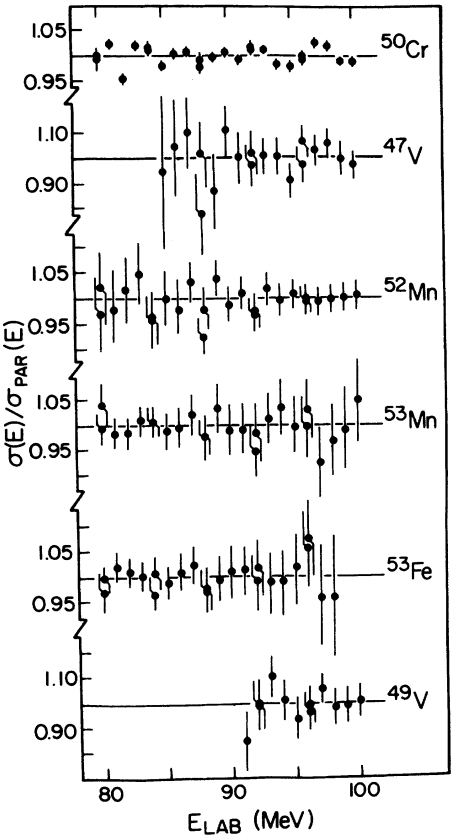

FIG. 10. The results of the gamma ray measurements of $^{28}Si + ^{28}Si$ fusion, presented as the ratio of the cross section to the average cross section determined by fitting a parabola to the data in a sliding 8 MeV interval.

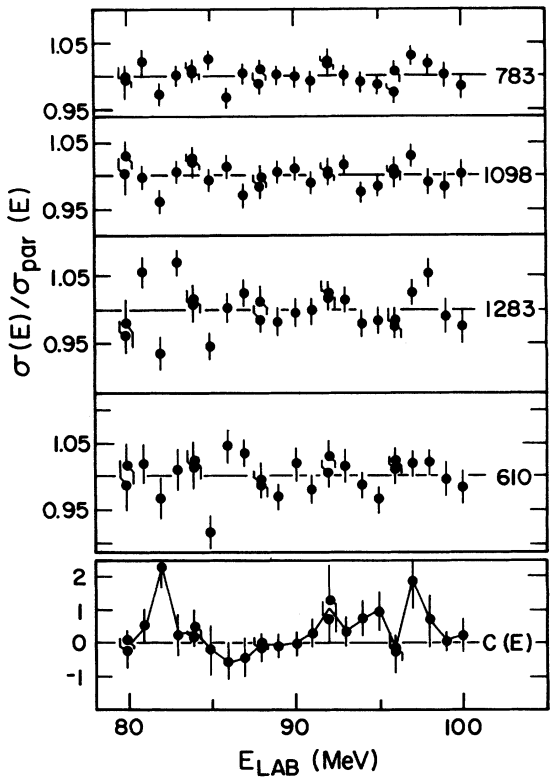

FIG. 11. A correlation analysis of the yields of four gamma rays from the yrast cascade of ^{50}Cr. A positive value of $C(E)$ indicates correlated behavior of the four yields at that energy.

with a smooth energy dependence. The yield of ^{50}Cr and, to a lesser extent, that of ^{47}V show some evidence for structure, over and above the envelope of the data. This is demonstrated more clearly in Fig. 10, which shows the ratio of the data to a parabolic fit for a sliding 8 MeV interval. The only channel showing significant deviation from smooth behavior is ^{50}Cr. The significance of this apparent structure in the ^{50}Cr channel may be tested by performing a correlation analysis of the cascade gamma rays in this nucleus. If the structure is real, the yield of each gamma ray should show the same structure. The results of such a correlation analysis are shown in Fig. 11, where the yields of four gamma rays in the yrast cascade of ^{50}Cr are shown together with the cross correlation function[11]

$$C(E)=\frac{2}{N(N-1)}\sum_{i>j=1}^{N}\frac{D_i(E)D_j(E)}{r_i(E)r_j(E)}\,, \tag{8}$$

where

$$r_i^{\,2}=\langle D_i^{\,2}(E)\rangle\,, \tag{9}$$

where the average is taken over the sliding 8 MeV interval and where

$$D_i(E)=\frac{\sigma_i(E)}{\langle\sigma_i(E)\rangle}-1\,. \tag{10}$$

The positive values of $C(E)$ near 92 and 97 MeV indicate the presence of correlated structures at these energies, as suggested by the data in Fig. 4. A similar analysis using randomly generated data shows, however, that there is an approximately 10% probability that the above result arises from purely random fluctuations. This analysis is therefore merely suggestive of the existence of real correlated structure, and a more detailed experiment is therefore required before a definitive statement can be made regarding these possible structures.

It is true, nevertheless, that the present results are consistent with expectations based on the sys-

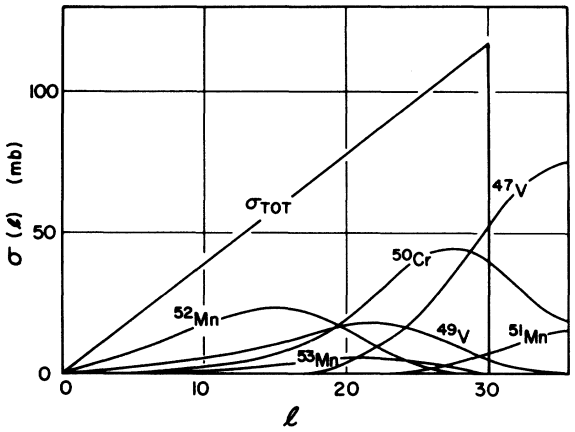

FIG. 12. Results of statistical model calculations described in the text showing the population of various final nuclei as a function of compound nucleus spin.

tematics of the fusion oscillations in lighter systems. Those systematics suggest that the resonancelike behavior may be associated with the highest partial waves leading to fusion, the advent of each successive partial wave giving rise to a bump in the fusion cross section. The relevant scaling parameter in determining the magnitude of the oscillations is, therefore, simply the ratio of the flux in the largest partial wave to the total flux contributing to fusion:

$$\frac{\sigma_l}{\sigma_{fus}} = \frac{(2l+1)\Delta l}{(l+1)^2} \approx \frac{2\Delta l}{l} \qquad (11)$$

and by extrapolating the magnitude of the fusion oscillation in $^{16}O + ^{16}O(l \sim 14)$ to $^{28}Si + ^{28}Si(l \sim 30)$ we expect a structure of at most 4% of the total cross section for fusion, consistent with the magnitude of the observed fluctuations in the yields of gamma rays from ^{50}Cr. Also consistent with the origin of this effect in the largest partial waves is the observation of structure in the yields of nuclei such as ^{50}Cr and ^{47}V, and not in other channels. Figure 12 shows the result of a statistical model calculation of the decay of ^{56}Ni at an excitation energy of 61 MeV, which is appropriate to a $^{28}Si + ^{28}Si$ bombarding energy of 100 MeV. The triangle shows the sharp cutoff spin distribution in the compound nucleus, inferred from the total fusion cross section measured at this energy. The curves show the regions of angular momentum space which result in the population of each evaporation residue after neutron, proton, and alpha particle evaporation. The calculation was performed using the code CASCADE,[12] incorporating the standard parameters used as default options in the code; the calculations should therefore be taken as only qualitatively correct. It is nevertheless clear that the yields of nuclei like ^{50}Cr and ^{47}V, which result predominantly from the higher spin states of the compound nucleus, are likely to be much more sensitive to the energy dependence of the highest fusing angular momenta than are nuclei such as ^{52}Mn, which originate exclusively from the lower spin states of ^{56}Ni. These qualitative observations are in agreement with the experimental results and, together with the magnitude of the observed fluctuations, suggest a common physical origin of the effect in this system and in the lighter fusing systems. It is clear, however, that more experimental work is required before definite conclusions can be reached.

This work was supported by the U.S. Department of Energy.

*Present address: Bell Laboratories, Murray Hill, New Jersey 07974.

†Present address: Bell Laboratories, South Plainfield, New Jersey 07080.

[1]A recent compilation of fusion data of light systems may be found in D. G. Kovar, D. F. Geesaman, T. H. Braid, Y. Eisen, W. Henning, T. R. Ophel, M. Paul, K. E. Rehm, S. J. Sanders, P. Sperr, J. P. Schiffer, S. L. Tabor, S. Vigdor, B. Zeidman, and F. S. Prosser, Jr., Phys. Rev. C 20, 1305 (1979).

[2]L. R. Medsker, J. V. Theisen, L. H. Fry, Jr., and J. S. Clements, Phys. Rev. C 19, 790 (1970).

[3]P. Bonche, K. T. R. Davies, B. Flanders, H. Flocard, B. Grammaticos, S. E. Koonin, S. J. Krieger, and M. S. Weiss, Phys. Rev. C 20, 641 (1979).

[4]R. R. Betts, S. B. DiCenzo, and J. F. Petersen, Phys. Rev. Lett. 43, 253 (1979).

[5]A. Berinde, R. O. Dimitriu, M. Gresescu, I. Neaumu, C. Protop, N. Scintei, C. M. Simionescu, B. Heits, H. W. Schuh, P. VonBrentano, and K. O. Zell, Nucl. Phys. A284, 65 (1977); C. J. Lister, J. W. Olness, and I. P. Johnstone, Phys. Rev. C 18, 2169 (1978); J. W. Noé, R. W. Zurmühle, and D. P. Balamuth, Nucl. Phys. A277, 137 (1977); A. R. Poletti, B. A. Brown, D. B. Fossan, and E. K. Warburton, Phys. Rev. C 10, 2329 (1974); Z. P. Sawa, J. Blomqvist, and W. Gullholmer, Nucl. Phys. A205, 257 (1973); A. M. Stefanini, C. Signorini, M. Morando, and R. A. Ricci, Nuovo Cimento 33A, 460 (1976).

[6]D. Glas and U. Mosel, Nucl. Phys. A237, 429 (1975).

[7]S. B. DiCenzo, Ph.D. dissertation, Yale University, 1980 (unpublished).

[8]S. J. Krieger in *Proceedings of the European Physical Society Topical Conference on Large Amplitude Collective Nuclear Motions, Keszthely, Hungary, 1979* edited by A. Kiss, J. Nemeth, and J. Zimanyi (Central Research Institute for Physics, Budapest, 1979), p. 378.

[9]H. H. Gutbrod, W. G. Winn, and M. Blann, Nucl. Phys.

A213, 267 (1973); D. G. Kovar (private communication).
[10]S. E. Vigdor, D. G. Kovar, P. Sperr, J. Mahoney, A. Menchaca-Rocha, C. Olmer, and M. S. Zisman, Phys. Rev. C 20, 2147 (1979).
[11]D. Glas and U. Mosel, Phys. Lett. 788, 9 (1978).
[12]R. Bass, Nucl. Phys. A231, 45 (1974).